Quarkonium and charm production in media at LHCb

Jihyun Bhom
on behalf of the LHCb Collaboration

Institute of Nuclear Physics PAN, Cracow

14 May 2019

Outline

LHCb detector

1. Single arm spectrometer
2. Fully instrumented in the forward region, $2 < \eta < 5$.
3. Flexible trigger $\rightarrow$ able to trigger on low momentum objects.
4. Fixed target capability via gas injection (SMOG: System for Measuring the Overlap with Gas).

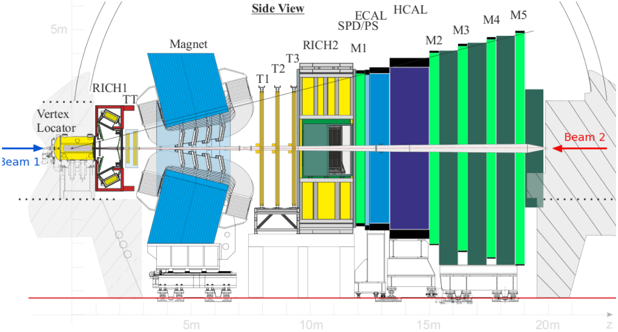

(a) Schematic view of the current LHCb detector [2014 JINST 9 P12005].

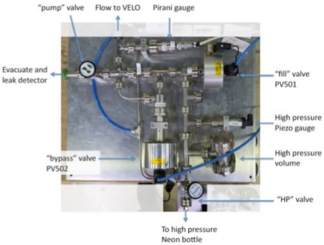

(b) The gas injection system installed near VELO.

- pPb: Forward production $(1.5 < y^* < 4.5)$
- Pbp: Backward production $(-5.5 < y^* < -2.5)$

Running modes and plan

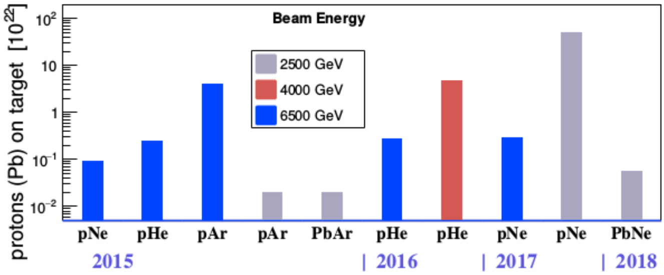

Element	He	Ne	Ar
A	4	20	40

In this talk;

- pHe $\sqrt{s_{NN}} = 86.6$ GeV $\rightarrow J/\psi$ and D^0 cross-section
- pAr $\sqrt{s_{NN}} = 110.4$ GeV $\rightarrow J/\psi$ and D^0 yield

Quarkonia production

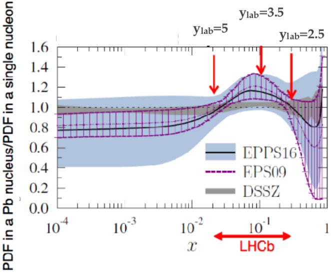

[Eur. Phys. J. C (2017) 77: 163]

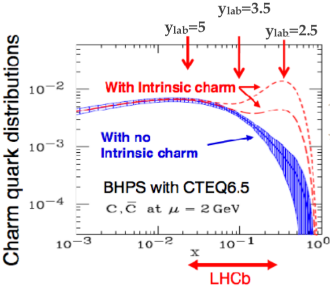

[Phys.Rev.D75:054029,2007]

Cold nuclear matter (CNM) effects

- Nuclear effects on parton densities (shadowing/antishadowing) $\rightarrow$ EPS09,EPPS16
- Coherent energy loss
- Quarkonia absorption by nucleons
- Comovers model
- Saturation: Color Glass Condensate

Recent results

- 1. Charm Production in Fixed-Target program in pHe and pAr
  –[PHYS. REV. LETT.122 (2019) 132002]
- 2. $\Upsilon(nS)$ in pPb at $\sqrt{s_{NN}} = 8.16$ TeV
  –[JHEP11(2018)194]

Charm Production in $\sqrt{s_{NN}} = 86.6$ GeV pHe

[PHYS. REV. LETT.122 (2019) 132002]

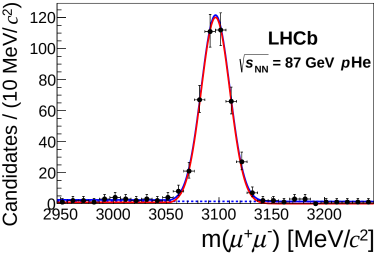

Mass distributions $J/\psi \rightarrow \mu^- \mu^+$.

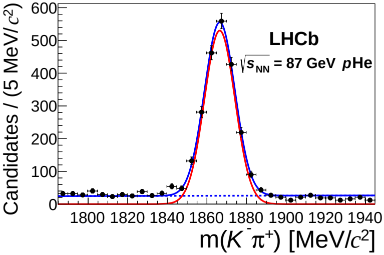

Mass distributions $D^0 \rightarrow K^- \mu^+$.

Crystal ball function (J/ψ) + an exponential function (background)
- Gaussian functions (D^0) + an exponential function (background)
- The dashed blue line corresponds to the combinatorial background, the red line to the signal, and the solid blue line to the sum of the two.

J/ψ and $c\bar{c}$ cross-section

[PHYS. REV. LETT.122 (2019) 132002]

- J/ψ and $c\bar{c}$ in pHe total cross-sections per target nucleon, in the full phase-space, are found to be:

  $\sigma_{J/\psi} = 1225.6 \pm 100.7 \; nb/nucleon$

  $\sigma_{D^0} = 156.0 \pm 13.1 \; \mu b/nucleon$

- Scaling D^0 cross-section with the global fragmentation ratio $f(c \to D^0) = 0.542 \pm 0.024$, production cross section can be obtained:

  $\sigma_{c\bar{c}} = 288 \pm 24.2(stat.) \pm 6.9(syst.) \; \mu b/nucleon$

J/ψ and $c\bar{c}$ cross-section

[PHYS. REV. LETT.122 (2019) 132002]

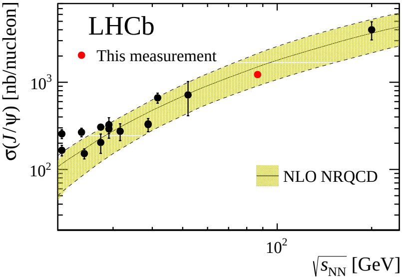

J/ψ cross-section measurements. The band corresponds to a fit based on NLO NRQCD.

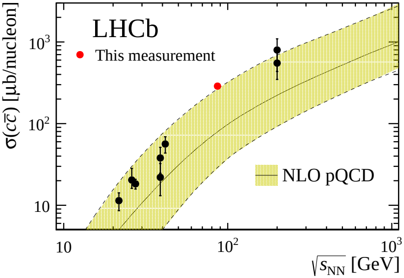

$c\bar{c}$ cross-section measurements. The band corresponds to NLO pQCD.

- Experimental data, represented by black points, are taken from NLO NRQCD (a), NLO pQCD (b).
- Good agreement with the theoretical calculations.

J/ψ and $c\bar{c}$ cross-section in $\sqrt{s_{NN}} = 86.6$ GeV pHe

[PHYS. REV. LETT.122 (2019) 132002]

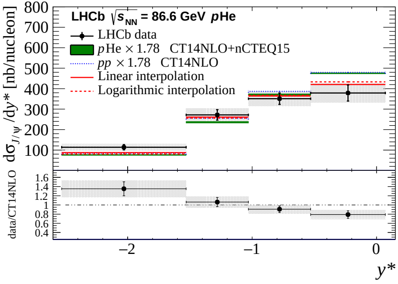

Differential J/ψ cross sections for pHe as a function of center-of-mass rapidity y^*.

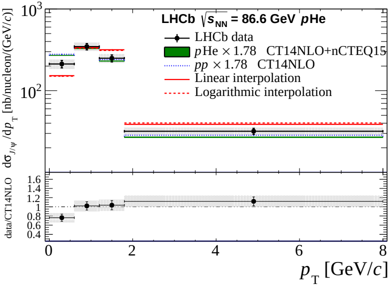

Differential J/ψ cross sections for pHe as a function of transverse momentum p_T.

- J/ψ and D^0 production cross sections in the rapidity range [2, 4.6].

$$\sigma^{86.8GeV}_{J/\psi} = 652 \pm 33(stat.) \pm 42(syst.)\ nb/nucleon$$
$$\sigma^{86.8GeV}_{D^0} = 80.8 \pm 2.4(stat.) \pm 6.3(syst.)\ \mu b/nucleon$$

- The lower panel of each plot shows the ratio of data to HELAC-ONIA scaled 1.78 pp predictions.
- Data are also compared with phenomenological parametrizations, interpolated to the present data energies.
- Solid and dashed red lines are obtained with linear and logarithmic interpolations, between the results from the E789, HERA-B and PHENIX.

D^0 cross-section in $\sqrt{s_{NN}} = 86.6$ GeV pHe

[PHYS. REV. LETT.122 (2019) 132002]

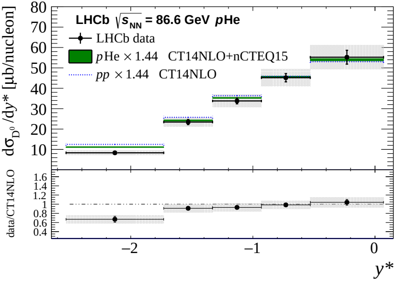

Differential D^0 cross sections for pHe as a function of center-of-mass rapidity y^*.

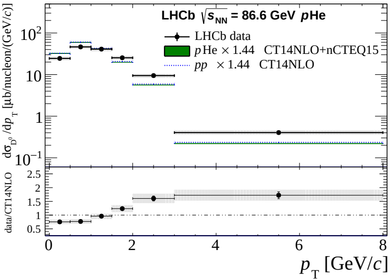

Differential D^0 cross sections for pHe as a function of transverse momentum p_T.

- The lower panel of each plot shows the ratio of data to HELAC-ONIA scaled 1.44 pp predictions.
- The HELAC-ONIA predictions underestimate the measured total cross section.
- The HELAC-ONIA predictions are rescaled by a factor 1.44 to compare the shape of the distributions.

J/ψ yield in $\sqrt{s_{NN}} = 110.4$ GeV pAr

[PHYS. REV. LETT.122 (2019) 132002]

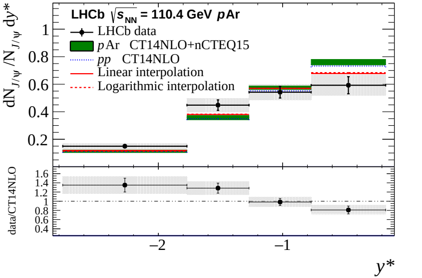

Differential J/ψ yield for pAr as a function of center-of-mass rapidity y^*.

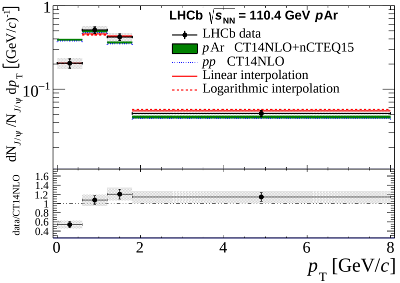

Differential J/ψ yield for pAr as a function of transverse momentum p_T.

- The lower panel of each plot shows the ratio of data to HELAC-ONIA pp predictions.
- Data are also compared with phenomenological parametrizations, interpolated to the present data energies.
- Solid and dashed red lines are obtained with linear and logarithmic interpolations, between the results from the E789, HERA-B and PHENIX.

D^0 yield in $\sqrt{s_{NN}} = 110.4$ GeV pAr

[PHYS. REV. LETT.122 (2019) 132002]

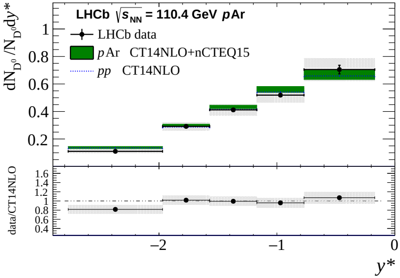

Differential D^0 yield for pAr as a function of center-of-mass rapidity y^*.

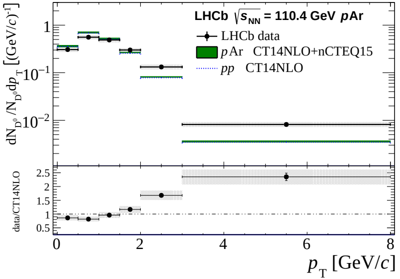

Differential D^0 yield for pAr as a function of transverse momentum p_T.

- The lower panel of each plot shows the ratio of data to HELAC-ONIA pp predictions.
- The HELAC-ONIA predictions underestimate the measured total cross section.

Study of $\Upsilon(nS)$ in pPb collisions at $\sqrt{s_{NN}} = 8.16$ TeV

- [JHEP11(2018)194]

1. $p_T > 1$ GeV/c and $2.0 < \eta < 5.0$
2. Crystal Ball functions ($\Upsilon(nS)$) + exponential function (background)
3. Yields of $\Upsilon(1S)$, $\Upsilon(2S)$, $\Upsilon(3S)$ mesons in Pbp and pPb as given by the fit.

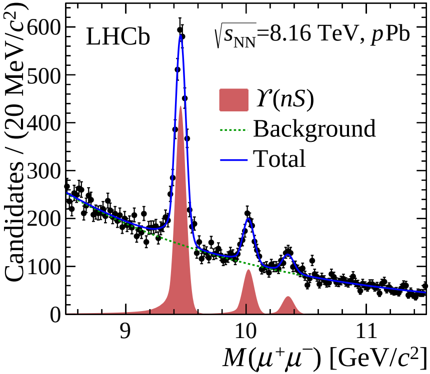

Invariant-mass distribution of $\mu^+\mu^-$ pairs.

Samples	$1S$	$2S$	$3S$	$\mathcal{L}$
pPb	2705 ± 87	584 ± 49	262 ± 44	12.5 nb^{-1}
Pbp	3072 ± 82	679 ± 54	159 ± 39	19.3 nb^{-1}

Yields of $\Upsilon(nS)$. The uncertainties are statistical only.

Study of $\Upsilon(nS)$ in pPb collisions at $\sqrt{s_{NN}} = 8.16$ TeV

- [JHEP11 (2018) 194]

The total $\Upsilon(nS)$ cross-sections;

$$\sigma^{\Upsilon(1S)}_{pPb} = 22.8 \pm 0.9(stat) \pm 2.1(syst)\mu b$$
$$\sigma^{\Upsilon(2S)}_{pPb} = 6.4 \pm 0.6(stat) \pm 0.8(syst)\mu b$$
$$\sigma^{\Upsilon(3S)}_{pPb} = 2.5 \pm 0.4(stat) \pm 0.3(syst)\mu b$$
$$\sigma^{\Upsilon(1S)}_{Pbp} = 20.3 \pm 0.8(stat) \pm 2.6(syst)\mu b$$
$$\sigma^{\Upsilon(2S)}_{Pbp} = 6.0 \pm 0.5(stat) \pm 0.9(syst)\mu b$$
$$\sigma^{\Upsilon(3S)}_{Pbp} = 1.2 \pm 0.3(stat) \pm 0.2(syst)\mu b$$

The production of both $\Upsilon(1S)$ and $\Upsilon(2S)$ is suppressed in the forward pPb region with respect to the scaled value from pp, as already observed in the prompt J/ψ measurement [Phys. Lett. B 740 (2015) 105].

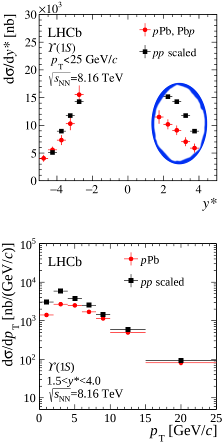

Cross-section of $\Upsilon(1S)$

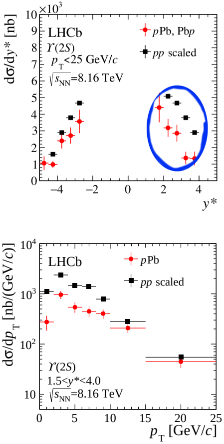

Cross-section of $\Upsilon(2S)$

Study of $\Upsilon(nS)$ in pPb collisions at $\sqrt{s_{NN}} = 8.16$ TeV

- [JHEP11 (2018) 194]

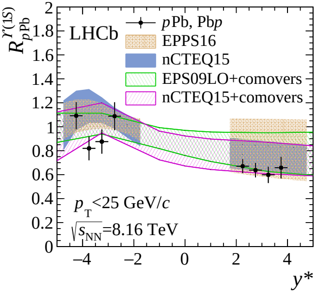

Nuclear modification factors of the $\Upsilon(1S)$ mesons

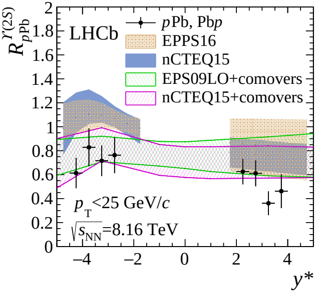

Nuclear modification factors of the $\Upsilon(2S)$ mesons

-The bands correspond to the theoretical predictions for the nCTEQ15 and EPPS16 nPDFs sets, and the comovers model.

- The nuclear modification factor for ^{208}Pb;

$$R_{pPb}(p_T, y^*) = \frac{1}{208} \frac{d^2\sigma_{pPb}(p_T, y^*)/dp_T dy^*}{d^2\sigma_{pp}(p_T, y^*)/dp_T dy^*}$$

pp interpolated to $\sqrt{s} = 8.16$ TeV using the LHCb at $\sqrt{s} = 2.76$, 7, 8, and 13 TeV.

Study of $\Upsilon(nS)$ in pPb collisions at $\sqrt{s_{NN}} = 8.16$ TeV

- [JHEP11 (2018) 194]

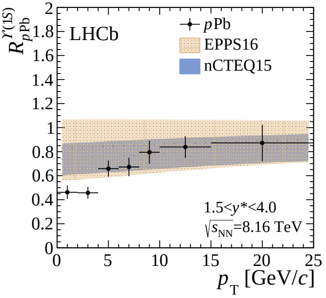

Nuclear modification factors of the $\Upsilon(1S)$ mesons

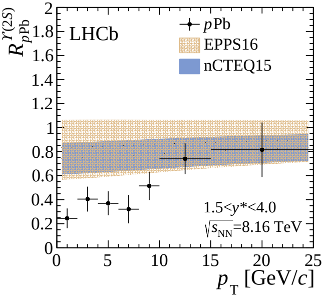

Nuclear modification factors of the $\Upsilon(2S)$ mesons

- The bands correspond to the theoretical predictions for the nCTEQ15 and EPPS16 nPDFs sets.

Study of $\Upsilon(nS)$ in pPb collisions at $\sqrt{s_{NN}} = 8.16$ TeV

- [JHEP11 (2018) 194]

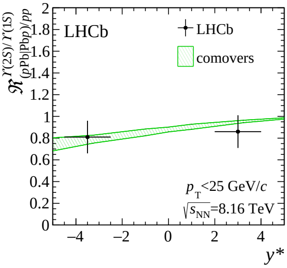

Double ratios for $\Upsilon(2S)$ over $\Upsilon(1S)$.

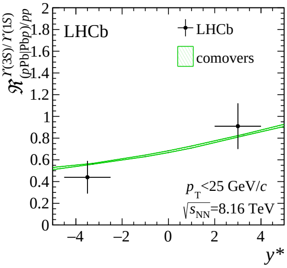

Double ratios for $\Upsilon(3S)$ over $\Upsilon(1S)$.

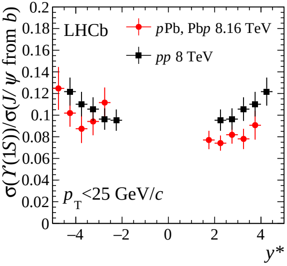

Ratio of $\Upsilon(1S)$ to nonprompt J/ψ cross-sections.

- For the double ratio of the $\Upsilon(3S)$ over $\Upsilon(1S)$ in the backward a clear indication of stronger suppression is observed, in agreement with the comovers model.
- Integrated Double Ratios;

$$\mathfrak{R}^{\Upsilon(3S)/\Upsilon(1S)}_{pPb/pp} = 0.81 \pm 0.15, \ \mathfrak{R}^{\Upsilon(2S)/\Upsilon(1S)}_{pPb/pp} = 0.86 \pm 0.15$$
$$\mathfrak{R}^{\Upsilon(3S)/\Upsilon(1S)}_{Pbp/pp} = 0.44 \pm 0.15, \ \mathfrak{R}^{\Upsilon(2S)/\Upsilon(1S)}_{Pbp/pp} = 0.91 \pm 0.21$$

- The ratio of the $\Upsilon(1S)$ and nonprompt J/ψ (J/ψ coming from b-hadron decays) cross-sections in pPb and Pbp is measured, where the nonprompt J/ψ cross-section was measured previously by LHCb same data sample.

Conclusion

- 1. The first measurement of heavy flavor production in fixed-target configuration at the LHC.
  pHe $\sqrt{s_{NN}} = 86.6$ GeV $\rightarrow J/\psi$ and D^0 cross-section
  pAr $\sqrt{s_{NN}} = 110.4$ GeV $\rightarrow J/\psi$ and D^0 yield
  $\rightarrow$No evidence for a substantial intrinsic charm content of the nucleon is found.

- 2. The production of $\Upsilon(nS)$ states is studied in pPb collisions at $\sqrt{s_{NN}} = 8.16$ TeV.
  The results are consistent with previous observations and
  with the theoretical calculations, indicating a suppression of $\Upsilon(nS)$ production in pPb.

Backup

The Fixed Target data taking (SMOG)

- SMOG: System for Measuring the Overlap with Gas

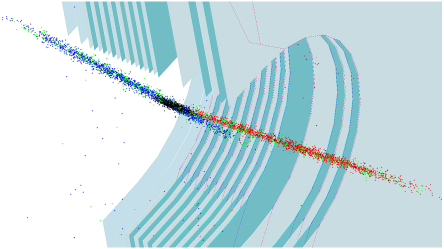

As the beam passes through LHCb, interactions with gas allow the experiment to measure the full beam profile. In this diagram, neon gas, beam 1 (blue) and beam 2 (red) are measured by the surrounding VELO detector.
https://cds.cern.ch/journal/CERNBulletin/2015/47

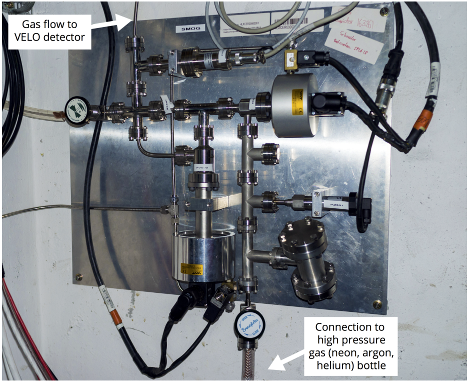

The gas injection system installed near the VELO detector at LHCb.

Introduction of fixed target mode with LHCb

p-Gas and Pb-Gas data taking.

http://cerncourier.com/cws/article/cern/68420

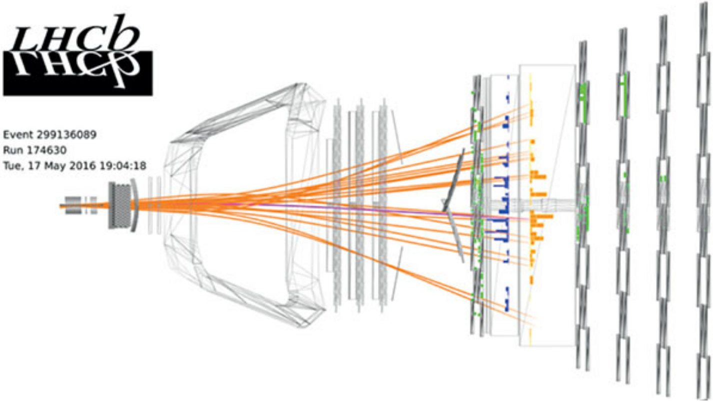

Event simulation in pHe

- A fully reconstructed protonhelium collision event in the LHCb detector, with the particle identified as an antiproton.